Multi-Pass Friction Stir Lap Welding of AA 6061-T6: Implication of Tool Pin Overlapping on Microstructure and Mechanical Properties of Joints

Tanmoy Medhi[1] , Ankan Das[1] , Pardeep Pankaj[1] , Sajan Kapil[1] , Pankaj Biswas[1]

[1] IIT Guwahati, Department of Mechanical Engineering, Assam, India.

Abstract: The present study focuses on the influence of a 5-pass overlapped friction stir lap welding of AA6061-T6 on the mitigation of defects and its simultaneous effect on microstructure and mechanical properties. Tool pin overlapping percentage of 0%, 25%, 50% and 75% was employed, from which it was observed that defects significantly reduced at higher overlapping. Fine equiaxed grains were observed across all the nugget zones in both top, and bottom regions were developed due to simultaneous overlapped passes; the grain size of which varied from 8.5 μm to 3.5 μm. The grains became finer, which increased of overlapping percentage. The microhardness of the processed zone was significantly reduced during overlapping that varied from a range of 43 $HV_{0.1}$ to 49 $HV_{0.1}$ as compared to base metal which was interpreted due to changes in grain size and secondary precipitate distribution during overlapping. A maximum ultimate tensile strength of 230 MPa was achieved at 50% overlapping, whereas minimum ultimate tensile strength of 160 MPa was achieved at 0% overlapping. Fractography of fracture surface showed a ductile failure at 50% that showed a number of dimples of varying shapes and sizes.

Key-words: Friction stir lap welding; Multi-pass weld; Overlapping; AA 6061-T6; Microstructure; Mechanical properties.

1. Introduction

Due to its attractive properties, such as high strength to weight ratio, formability, fatigue, corrosion resistance, and comparatively lower cost, AA 6061-T6 is considered a high-performing structural material [1,2]. This has led to its wide usage in structural manufacturing industries like aerospace, shipbuilding, and automotive for high demanding applications [3,4]. Aluminium alloys are mainly joined by friction stir welding (FSW) due to its solid-state way of joining that was developed and patented by The Welding Institute (TWI) in the year 1991 [5]. Since then, FSW has come up a long way and is highly developed, due to which it has become a prime process in industries, as discussed before.

Though the main focus is given to butt joints of FSW, the friction stir lap welding (FSLW) joints are equally important, especially in the area of load-bearing capacities of the joints. It is reported that in an aircraft, the stringers are used to strengthen plane panels, floor decks, and frames of wings, the profiles of which are always FSLW to the outer skin [6-8]. In automotive sectors, frames of an engine, cooling elements, rims of wheel and heat exchangers, etc., all involve FSLW [9]. Also, the FSLW joints are a suitable replacement for the rivet joints, which results in a reduction in cost and production time, and related defects [10].

The main characteristic of a lap joint that makes it interesting as well as peculiar from butt joints is the existence of a crack-like unbonded surface near the interface that is inevitable, which is termed as hooking [11]. Also, another imperfection that exists during FSLW is the kissing bond, which is also termed cold lap [12]. These two imperfections act as stress concentration sites and are commonly responsible for the failure of lap joints [7,13,14]. The appearance of these features and characteristics of microstructure and mechanical properties are controlled by welding process parameters and conditions [15-17]. Several researches related to FSLW that discuss these variations and control mechanisms are reported, but all are mainly focussed on a single pass or single track FSLW [18-22]. However, lately, the focus is slowly shifting towards research related to multi-pass or multi-track FSLW. It is reported that the multi-track FSLW strategy acts as a defect repairing method as well as increases the bonded area that may help in improving the strength of the joint [23-25]. This is a requirement from the present scenario of industry 4.0, which will indicate the manufacturing community about the overall performance of the system [26]. If we consider a multi-pass strategy, the weld surface will consist of overlapped passes, i.e., consecutive weld passes will overlap the previous one. This will, in turn, create an overlapping of the microstructure, which is an important phenomenon to study as the simultaneous overlapping passes also varies the microstructure and mechanical properties of the nugget zone [27-29].

Multi-pass friction stir lap welding of AA 6061-T6: implication of tool pin
overlapping on microstructure and mechanical properties of joints

Medhi et al.

Moreover, this strategy has a high potentiality for large-scale fabrication of monolithic aluminum components that is also a basic technology or foundation that will help in the research and development of friction stir additive manufacturing (FSAM) [30-33]. Apart from this, the multi-pass FSLW may also be applied as a prospective route for the fabrication of aluminum-based bimetal clad plates [34,35]. The works of literature related to multi-track FSLW of aluminum alloys are limited, due to which there is an utmost requirement of understanding the evolution of microstructure and mechanical properties during the process. This will provide meaningful exploration in this area for further research.

The present work focuses on providing a fundamental insight interpretation of the various weld characteristics of FSLW of AA 6061-T6 alloy by varying the overlapping percentage while following a multi-pass strategy.

2. Materials and Methods

Multi-pass friction stir lap welding of 4 mm thick AA 6061-T6 plates (85 $HV_{0.1}$, 307 MPa UTS) and dimensions of 200 mm×150 mm was fabricated using an FSW machine at a constant rotational speed of 600 rpm, traverse speed of 70 mm/min, tool tilt angle of 1.5° and a shoulder plunge depth of 0.2 mm was maintained throughout the welding in order to minimize excessive penetration of pin in the lower sheet and flashing out of the material. The welding was carried out using a tool made of H-13 tool steel and composed of a concave shoulder of 17 mm diameter, the tapered pin of 6 mm root diameter and 4 mm tip diameter, and 5 mm height (Figure 1). Tool steel is used here as it is the most commonly used material in FSW as it is economical, easily available, has better machinability, and well-accepted material characteristics [36]. The H-13 tool steel is a hot-worked chromium-molybdenum air-hardened steel which is significant because of its high-temperature strength, fatigue, and wear resistance [36]. A tapered pin tool was used as it aids in enhancing the hydrostatic pressure in the weld zone that promotes the material stirring in the nugget [37]. Also, a tapered pin without thread is used to understand the material flow as a baseline [37]. The motion of the pin promotes the downward and upward movement of material in the front and rear sides, respectively, which maintains uniform properties across the thickness of the weld [38].
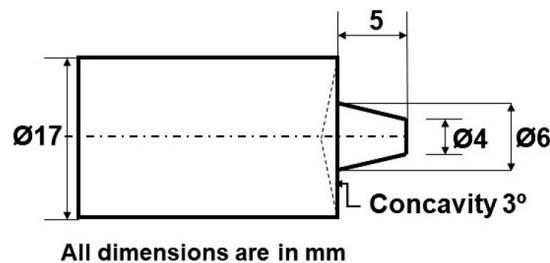

Figure 1. Schematic diagram of tool.

The multi-pass lap welding was accomplished by carrying out five passes, the schematic of which is shown in Figure 2a. As the primary aim of this study is to analyze the effect of overlapping percentages, so it is considered as a variable. An overlapping pin ratio (ORp) of 0%, 25%, 50%, and 75% is considered here, the schematic of which is shown in Figure 2b-e. The 0% ORp was used for the study as the minimum/no overlap of the pin, and 75% ORp is assumed to be maximum overlap, and the changes corresponding to the varying overlap of the pin were reported. This ratio helps in deciding the distance between two successive passes during the welding that can also be termed as overlapping length. The ORp is normally calculated by using the Formula 1 [39],

$$ORp = 1 - \frac{L}{D} \tag{1}$$

where L is the overlapping length, D is the pin diameter. The welding was started from AS in a manner such that after completion of the 1st pass, the tool pin was offset towards the RS by a distance corresponding to the respective L for varying ORp, which continued till the 5th pass. The passes were simultaneously carried out one after the other without any cooling. As discussed before, in order to focus on the primary aim of the study, these parameters were kept constant, and only ORp is varied.
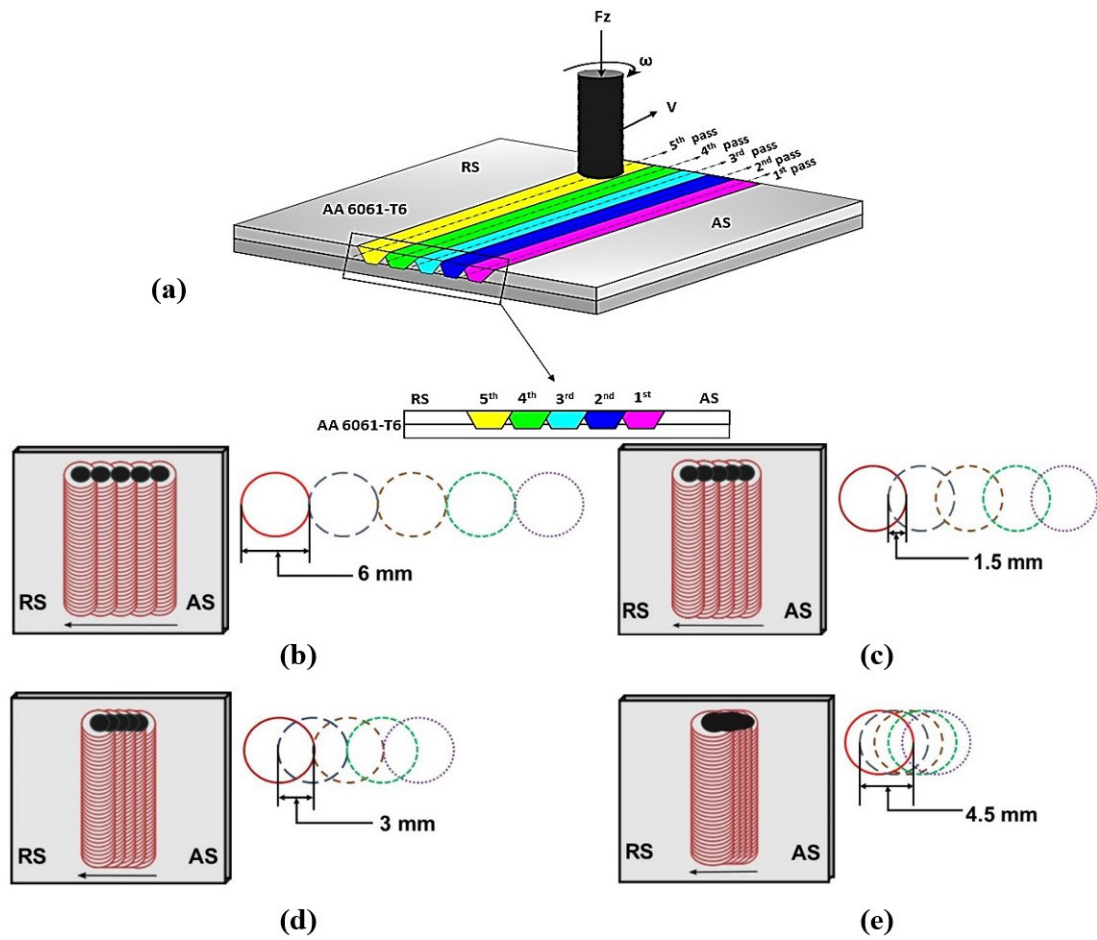
Multi-pass friction stir lap welding of AA 6061-T6: implication of tool pin
overlapping on microstructure and mechanical properties of joints

Medhi et al.

Figure 2. Schematic of (a) multi-pass strategy; pin overlapping percentage of (b) 0%, (c) 25%, (d) 50% and (e) 75%.

Following the welding, various samples were extracted from the weldment by using WEDM in the required shape and dimension of the samples for metallographic and metallurgical analysis. The samples for metallographic analysis were prepared by polishing till 2000 grade emery paper followed by alumina and colloidal silica polishing. The polished samples were then etched by using Keller's reagent in order to reveal the microstructure. The macrostructure and microstructure of the samples were observed by a Stereo zoom microscope, and Carl Zeiss made an upright optical microscope, respectively. The grain size was measured in both top, and bottom regions of each nugget developed due to respective passes by line-intercept technique as per ASTM E 112-12. The microhardness was recorded across the cross-section by an Omnitech Vickers microhardness tester. The indentation was made at intervals of 0.5 mm across the cross-section and along five lines 1 mm apart from the shoulder surface to the interface at a load of 100 g for a dwell period of 10 s (Figure 3). The tensile test was carried in a Shimadzu Static UTM machine having a capacity of 100 kN at a strain rate of 0.5 mm/min. The fractography was carried out by Carl Zeiss Gemini 300 FESEM machine.
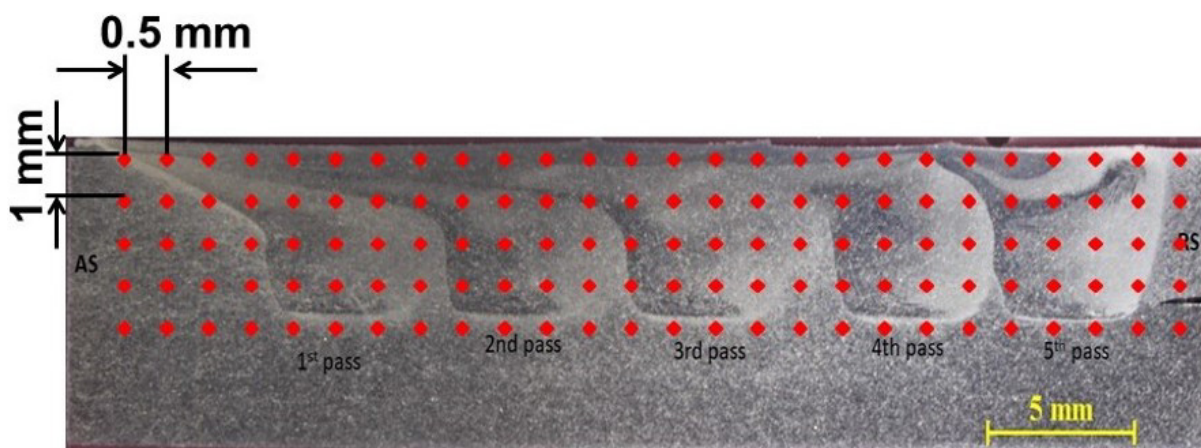

Figure 3. Specimen of hardness measurement.

Multi-pass friction stir lap welding of AA 6061-T6: implication of tool pin
overlapping on microstructure and mechanical properties of joints

Medhi et al.

3. Result and Discussion

3.1. Weld appearance and macrograph

The surface appearance and cross-sectional macrostructure at 0%, 25%, 50%, and 75% ORp are shown in Figure 4. All the cases generated a good surface appearance and were free from any surface defects. No flashes on the surface denoted that plunge depth considered was nominal, and the plasticized material was contained below the shoulder. The cross-sectional structure gives information about the degree of mixing in the nugget zone [40]. Distinct stacked onion rings in the form of dark bands (marked by black arrows) depicting a split pattern are observed in the nugget zone at 0%, 25%, and 50% ORp. It was termed as the split pattern as it existed in the form of stacked layers in the form of partial half ellipse-shaped bent patterns. These are also characteristic of material flow in the nugget zone that is affected by the shoulder, pin side surface, and pin bottom surface [41]. These dark bends of onion rings are prominent near the mid (towards AS) as well as the lower region of the nugget zone that denoting that the material flow is influenced by pin side surface as well as pin bottom surface. There tends to increase from 1st to 5th pass that denotes both the side and bottom surface of the pin, producing a good stirring effect on the area. Some certain changes are also observed in the shoulder-influenced zone, the thickness of which is represented by the distance between the shoulder surface and the intersection point on the nugget zone central axis of the line that is drawn to represent the flow arm in the AS. It is observed that the shoulder-influenced zone reduces from 1st to 5th pass for all the cases. It has been reported that the formation, as well as size of the nugget zone, depends on the displacement of material around the surface of the pin [42]. So as the shoulder influenced zone
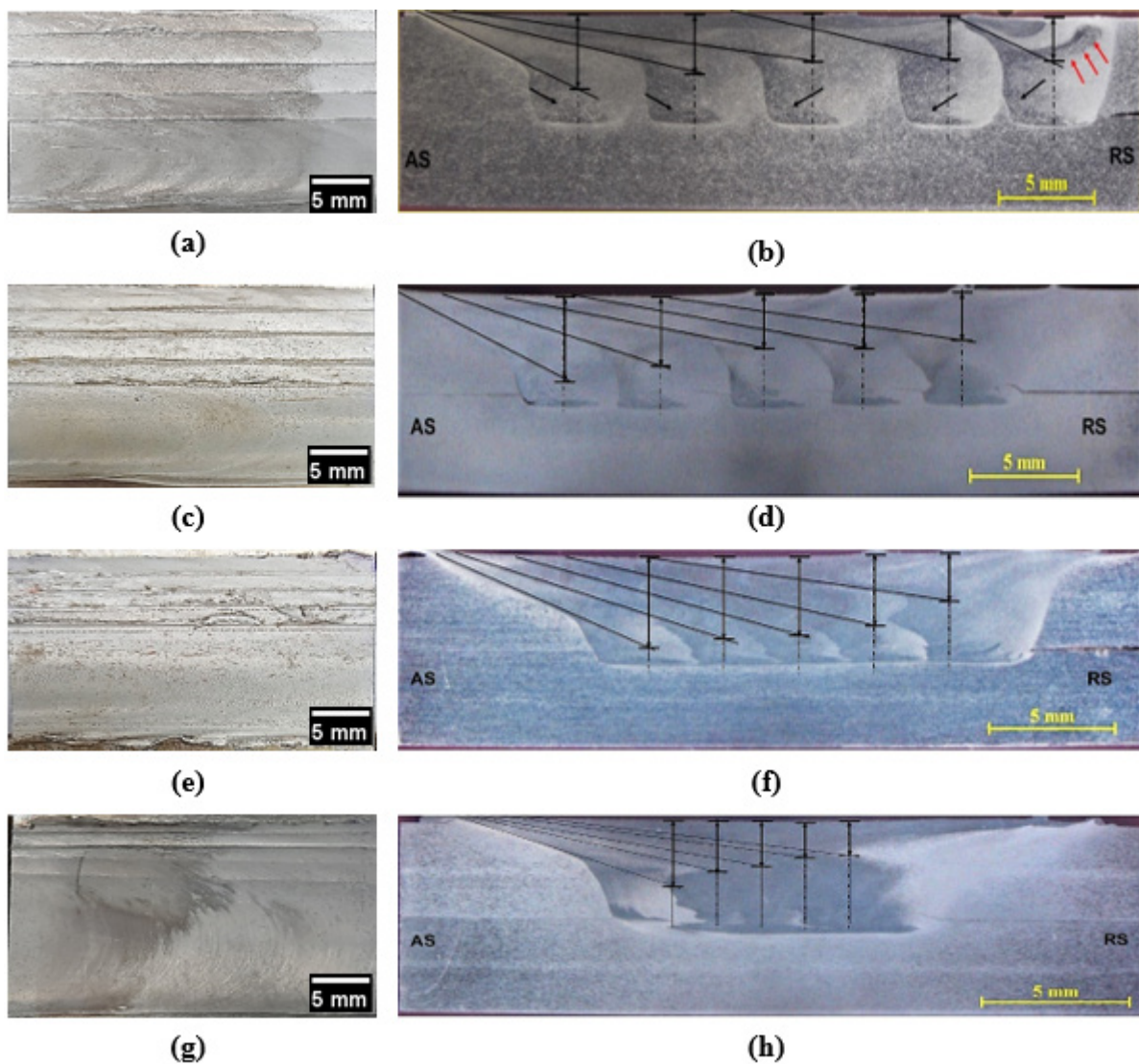
Figure 4. Weld surface appearance at (a) 0%, (c) 25%, (e) 50% (g) 75% and macrostructure at (b) 0%, (d) 25%, (f) 50% (h) 75% pin overlapping.

Multi-pass friction stir lap welding of AA 6061-T6: implication of tool pin
overlapping on microstructure and mechanical properties of joints

Medhi et al.

Decreases it can be said that the size or area of the nugget zone increases from 1st to 5th pass for all the cases, which means a better material consolidation around the tool pin is achieved with simultaneous passes.

However, the flow of dark bends tended to move upward with each pass, as marked by red arrows in the 5th pass at 0% up. This may be due to an increase in the upward extrusion force. This may be attributed due to the fact that as the number of passes increases, the area adjacent to the pass will be preheated, which will make the region softer. However, the flow of dark bends tended to move upward with each pass, as marked by red arrows in the 5th pass at 0% ORp. This may be due to an increase in the upward extrusion force generated by the action of the lower plate, which behaves as a backing plate for this study. Additionally, the upward flow will be facilitated through the stirring action of the pin surface. Moreover, as the number of passes increases, the region inside the SZ adjacent to each pass becomes soft since the succeeding pass acts as a preheating source. This leads to the easier upward flow of softened material but will be restricted at the top due to the forging effect of the rotating shoulder.

It was observed that when the ORp= 0%, the nugget zone of each pass did not fully overlap, but at maximum ORp, i.e., 75%, nearly all the nugget zones of each pass lay within the overlapping area, which also meant that the comparatively more overlapped area of shoulder region was achieved for all the passes. This led to an entirely different type of material flow that can be observed from the macrostructure. A clear absence of onion rings and the presence of swirl patterned flow (dark banded structures) is observed in the nugget zone. Such patterns indicate that the material flow is supported by both shoulder and pin profiles which is normally not seen during conventional FSLW. Such kind of flow is observed mainly during multi-pass overlapped friction stir processing, from which it can be said that as ORp increases, the final cross-section achieved is a processed region. The intensity of dark bands weakens from 1st to 5th pass, the lightest of which is observed in the RS, which may have occurred due to the displacement of the processed region from AS to RS with each pass [43]. Regarding the absence of the onion ring, it was suggested by Krishnan et al. [44] that this happens due to an increase in heat input during the process, which indicates that increasing the ORp from 0 to 75% will lead to a rise in heat input.

3.2. Microstructure

The microstructural changes at 0%, 25%, 50%, and 75% ORp is shown in Figure 5. Hooks accompanied by void defects are observed nearly for all the passes at 0% ORp. During lap welding, as the tool pin penetrates the lower sheet, the material extrusion is somewhat difficult due to the presence of oxide layers at the interface of the sheet. So as the pin penetration occurs, in addition to upward material extrusion into the nugget zone, material from the thermo-mechanical affected zone (TMAZ) will also have a tendency to flow upwards then, resulting in a hook. Voids are usually formed due to a lack of material transfer from the front to the rear side of the tool, as well as due to a shortage of heat input. Here is some extra material from the TMAZ that will flow upwards, so a cavity will be generated due to a lack of material to fill it, resulting in a void defect. Though hooks were present for all the passes, the voids diminished towards the 5th pass, which may be due to preheating of the region by the previous pass that led to better plasticization and flow of material. Some discontinuities along with micro-cracks (marked by black arrows) are observed near the interface that was periodically distributed. The presence of such defects may have occurred due to the use of a normal taper tool with no threads that reduced the material flow downwards. The hooks are an inevitable characteristic of lap joints, due to which it was observed at all the ORp. However, the appearance of void or discontinuities reduced as well diminished completely as the ORp increased. It was observed that at 25% ORp the discontinuities only appeared for the first two passes, whereas at 50% and 75%, there so was no evidence of the presence of any such defects. The defects were completely covered by the appearance of dense microstructure in the nugget zone. Also, as it was discussed before that, the heat input increases due to an increase of overlapping. This may have led to sufficient plastic deformation that supported a better material flow with each overlapping pass. This also suggests that even a simple taper tool with no threads can be used for FSLW if a properly overlapped multi-pass strategy is adopted.

Some light and dark zig-zag lines that are also termed as kissing bond defect was also observed in different degrees near the interface of the sheet (marked by yellow arrows). Such kind of defects usually occurs due to inadequate stretching of material near the pin that results in an insufficient breakage of oxide layers near the interface [45]. This is also a characteristic of insufficient pressure provided by the shoulder for the same. The zig-zag lines were slightly visible in a small area near the interface at 25% during the 1st pass and completely diminished and indistinguishable at 50% ORp. However, it was observed that at 75% ORp, a faint zig-zag line appeared during the 5th pass (marked by yellow lines). As the overlapping with simultaneous passes is very high so it can be said that nearly the same zone is getting processed several times. This will result in an excessive plastic deformation of the material, which may lead to sudden fluctuations in the contact condition of the tool with the workpiece, thereby affecting the contact pressure of the shoulder. Hence, the fluctuation in shoulder pressure may assist in the formation of these zig-zag lines. This suggests that controlling the ORp can lead to better material mixing at the interface as well as provide sufficient shoulder pressure for crushing the layers of oxides which in another sense is beneficial for reducing the kissing-bond defect during FSLW.
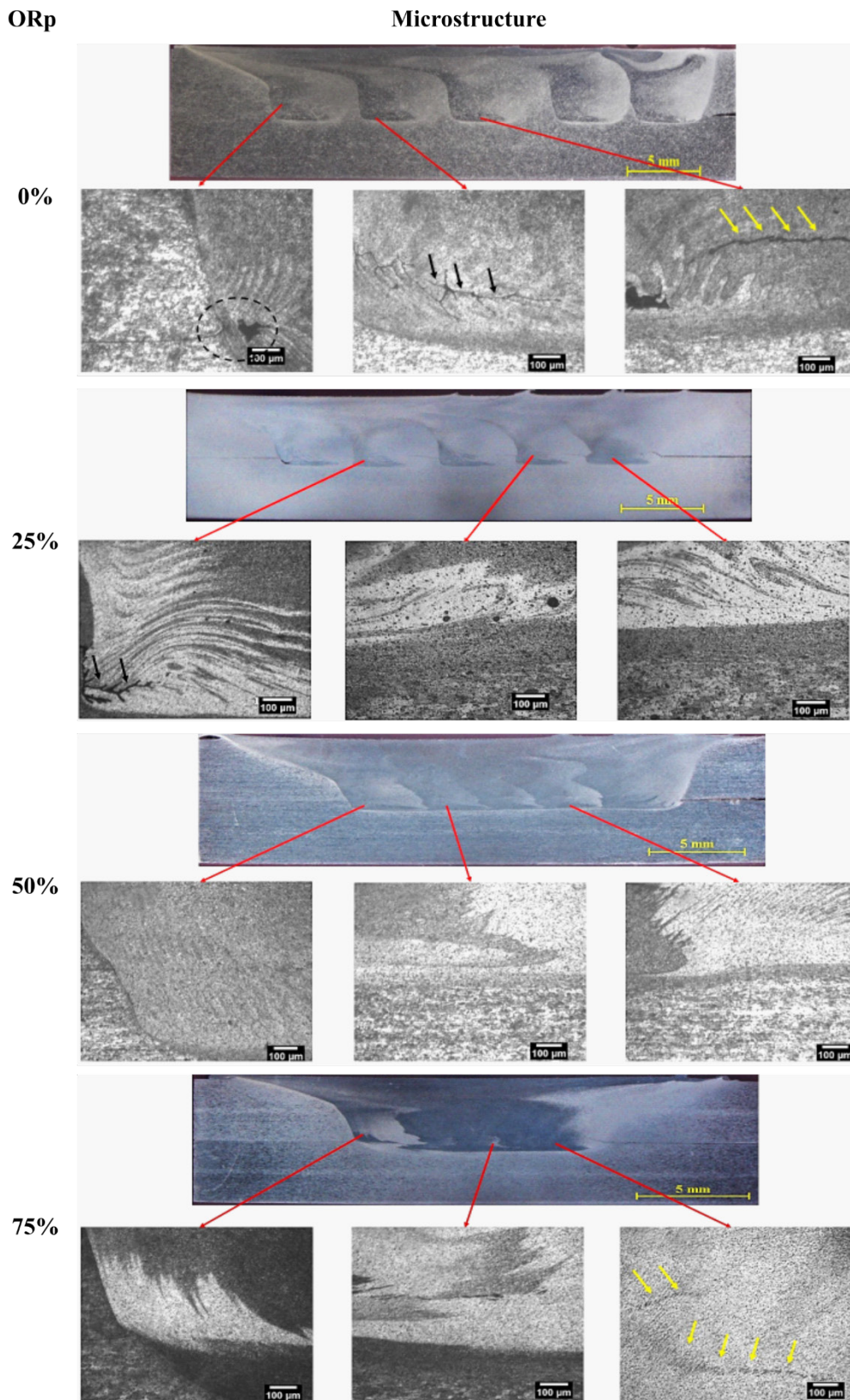
Multi-pass friction stir lap welding of AA 6061-T6: implication of tool pin overlapping on microstructure and mechanical properties of joints

Medhi et al.

ORp	Microstructure

Figure 5. Variation of microstructure at different ORp.

As discussed before, due to overlapping with multiple passes, the weldment generates a processed region that yields a dense microstructure. During FSLW, the plastic deformation of material induces dynamic recrystallization that leads to the formation of fine and equiaxed grains [46]. The variation in grains in the top and bottom region of similar locations at 0%, 25%, 50%, and 75% ORp is represented

Multi-pass friction stir lap welding of AA 6061-T6: implication of tool pin
overlapping on microstructure and mechanical properties of joints

Medhi et al.

in Figure 6. In order to see the complete variation, the grain size was measured at the top and bottom regions of each pass for different ORp, and the average distribution was plotted, which is shown in Figure 7. The grain distribution reveals that the variation is nearly uniform at the top and bottom regions of each pass for a particular ORp. This indicated that overlapping over each pass during welding will not bring any significant changes in grain size. However, the grains become finer with increasing ORp, which indicates that the percentage of overlapping will somewhat control the size of grains at different regions in the nugget zone. The average grain size in the top and bottom region of the nugget zone decreases from 8.5 μm and 5.6 μm to 4.7 μm and 3.5 μm respectively when the ORp increases from 0% to 75%. This may be attributed due to variation in strain rate as ORp increases. It is said that grain becomes finer at higher strain rates [47,48]. It was discussed before that at maximum ORp nearly the same material will be stirred and re-stirred again and again consecutively by each pass. This may lead to the generation of a high strain rate that may become a dominant factor in reducing the size of the grains. It is observed that the grains change from coarse to fine from top to bottom of the nugget zone. This may be attributed due to the abnormal growth of grains in these regions of the nugget zone [49]. The material deformation, as well as grain refinement in the top region of the nugget zone, is mainly controlled by the stirring action of the shoulder. As the shoulder is larger than the pin so it will generate more heat in the top region, thereby resulting in more heat input and a low cooling rate that will let the top region be exposed to more heat [50,51]. This will create an ambiance for the growth of grains. The bottom region is mainly deformed by the stirring action of the pin that creates swirls which are clearly observed from the microstructure. Also, the bottom region experiences lower thermal cycles, due to which a higher cooling rate occurs that reduces the nucleation time of the grain. This ensures that the bottom region will contain finer grains.
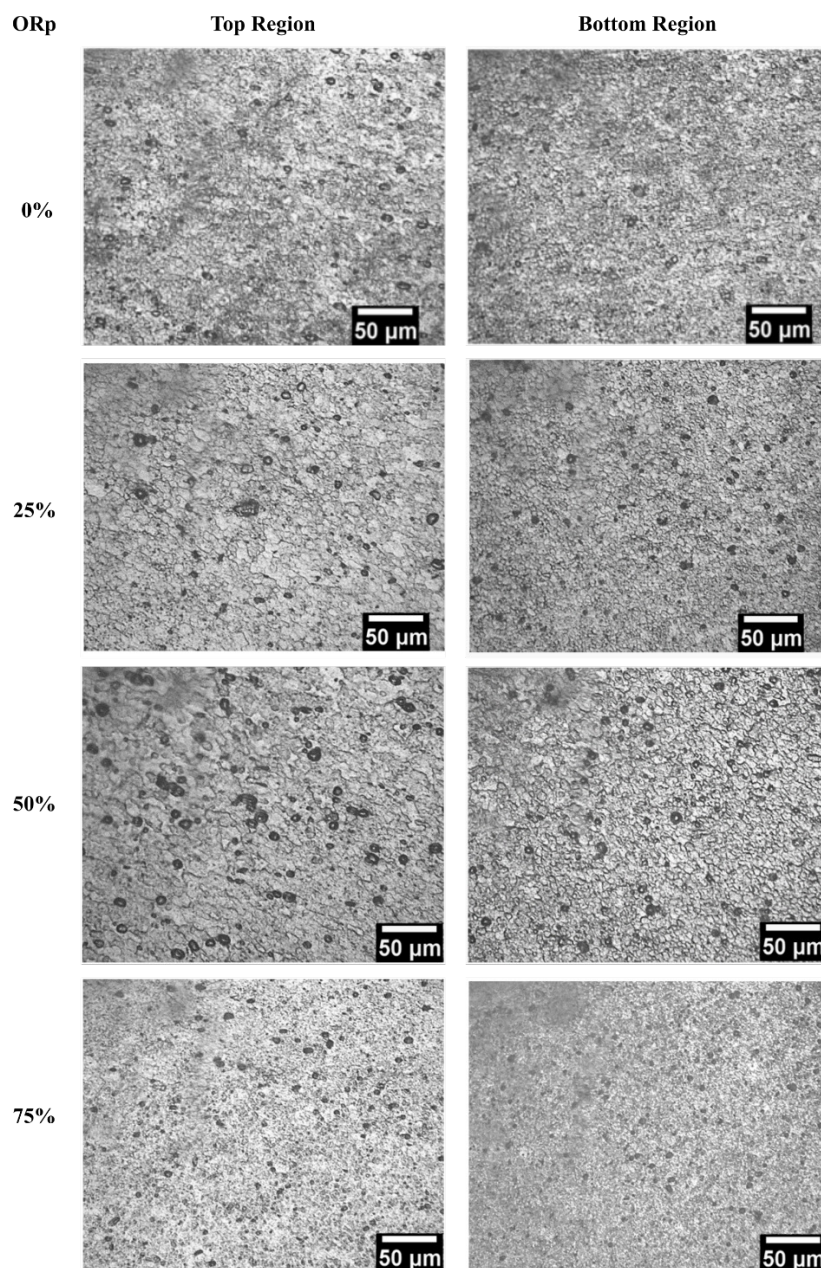
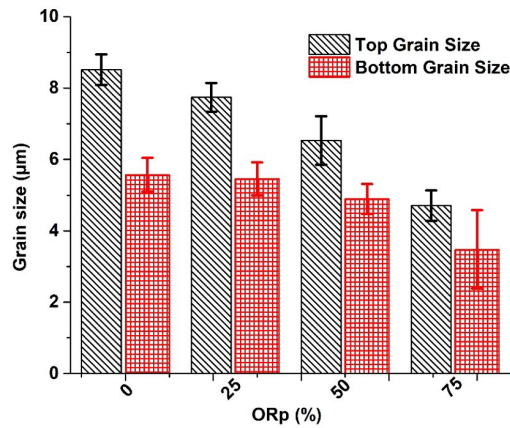**Figure 6.** Grains at top and bottom region of nugget for varying ORp.

Multi-pass friction stir lap welding of AA 6061-T6: implication of tool pin
overlapping on microstructure and mechanical properties of joints

Medhi et al.

Figure 7. Average grain size distribution for varying ORp.

3.3. Microhardness

The distribution of hardness exactly below the processed region along the cross-section of the weld for different ORp is represented in Figure 8. It is observed from the figure that a significant reduction in hardness along the cross-section takes place when compared with that of the base metal, which is around 84 $HV_{0.1}$. A non-uniform hardness distribution is observed along the nugget zone for all the samples. For different overlapping percentage, the hardness values are close but slightly increases in the nugget zone as the ORp increases. This clearly points out the effect due to variation in grain size. The grains were finest at 75% ORp as well as distributed uniformly in the nugget zone that may have yielded a comparatively higher hardness range. Very low hardness values ranging from 28 $HV_{0.1}$ to 38 $HV_{0.1}$ are recorded in the bottom region of the nugget zone for 0% and 25% ORp. This was due to indentation over a certain defect that was generated during welding for both the cases, defects which were clearly pointed out in the microstructure.
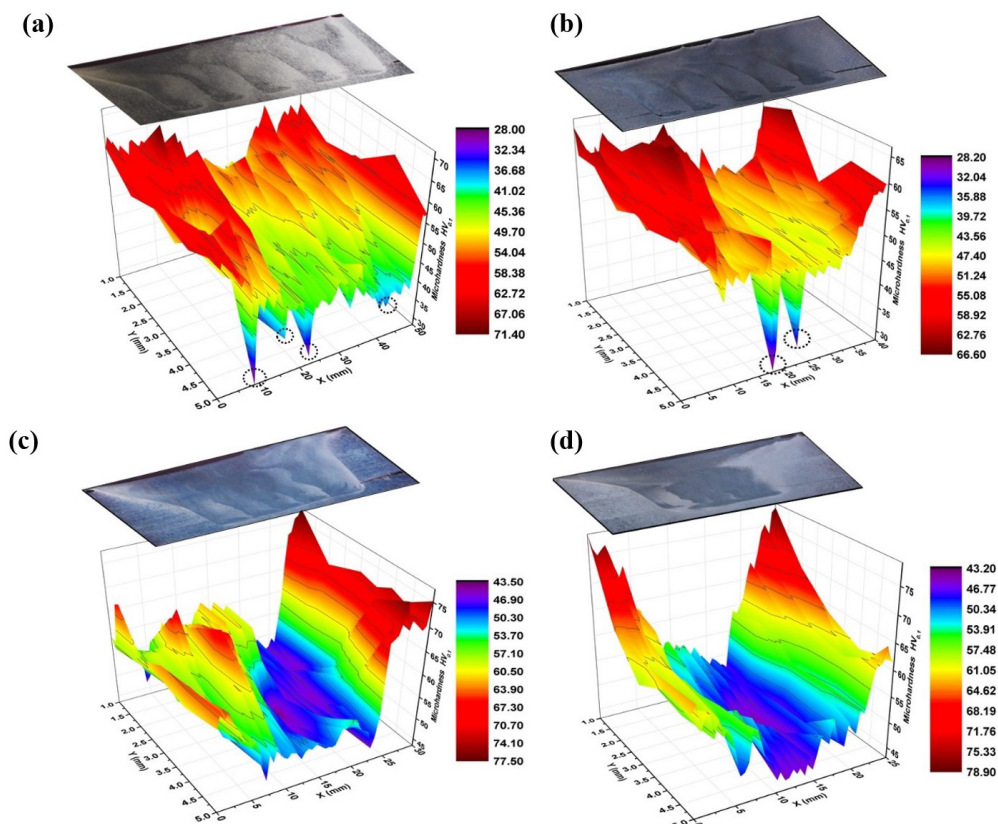

Figure 8. Microhardness mapping at (a) 0%, (b) 25%, (c) 50% and (d) 75%.

However, the distribution of hardness was somewhat different when it was recorded from 1st to 5th pass for each ORp (as shown in Figure 9). It has been reported earlier that severe.
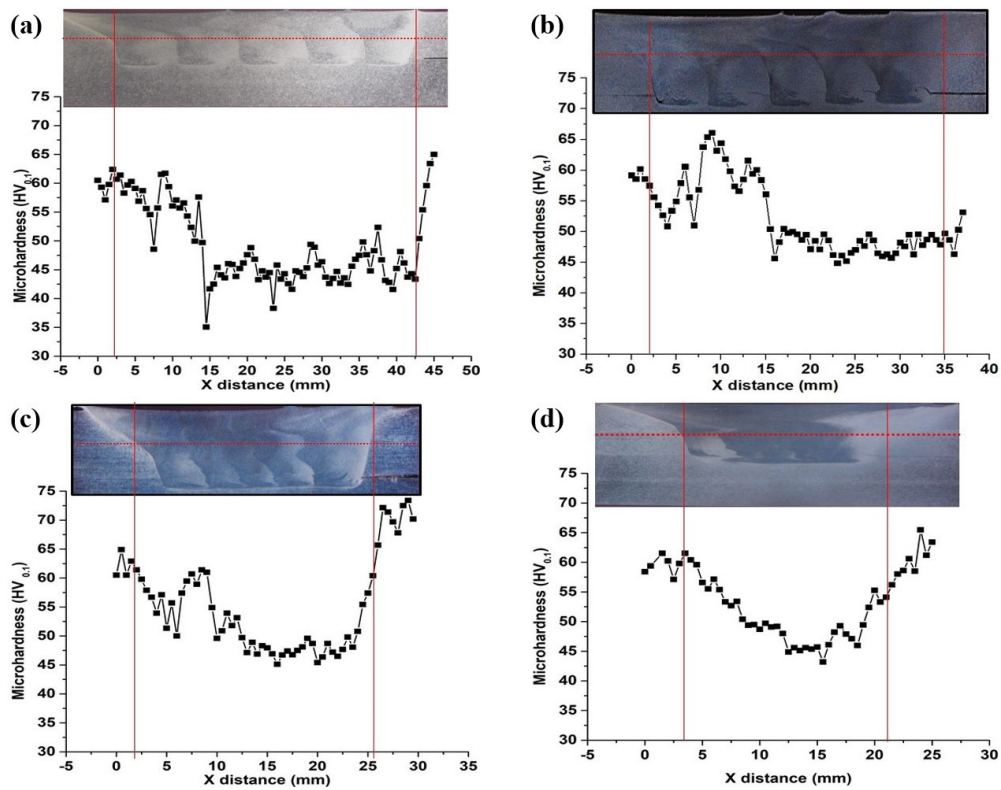
Multi-pass friction stir lap welding of AA 6061-T6: implication of tool pin
overlapping on microstructure and mechanical properties of joints

Medhi et al.

Figure 9. Microhardness variation along the centerline at (a) 0%, (b) 25%, (c) 50% and (d) 75%.

plastic deformation leads to the dissolution of secondary precipitates and phase particles in the case of aluminum alloys which get redistributed inside the grains [52]. During overlapping, from 1st to 5th pass the weld zone experiences processing multiple times, due to which a different level of dissolution of second phase particles (Mg_2Si particles) may have been achieved throughout the processed area. This leads to the random distribution of these particles due to the stirring action of the tool (Figure 10). This may be a probable reason for such overall lower and non-uniform hardness distribution in the nugget zone for different ORp.
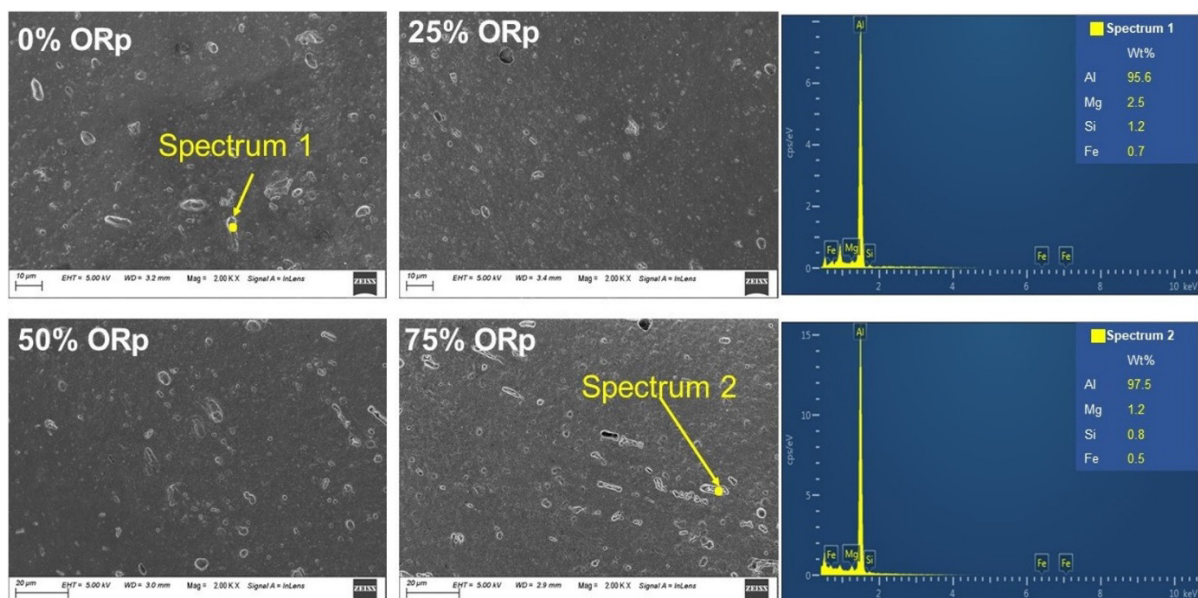

Figure 10. Secondary precipitates at varying ORp.

3.4. Tensile strength

The variation in the stress-strain curve for the transverse tensile test specimens at different ORp is shown in Figure 11a. As three samples were tested for each ORp for carrying out proper analysis, the variation of average UTS and YS with varying ORp

Multi-pass friction stir lap welding of AA 6061-T6: implication of tool pin overlapping on microstructure and mechanical properties of joints

Medhi et al.

is graphically represented and shown in Figure 11b. It is observed that the 50% ORp exhibits a maximum UTS of 230 MPa, which is about 74% of the base aluminum alloy. Below the 50% ORp, i.e., at 0% and 25% ORp, the UTS and elongation reduce, which can be attributed to the defect generation inside the nugget zone that may act as stress concentration sites and support crack propagation (Figure 5). Additionally, the coarse-grained microstructure in the nugget zone (Figure 6) may lead to the lower UTS of the 0% ORp than 50% ORp. It is clear that the test results are also in good agreement with the hardness, as the UTS increases for specimens having high hardness and fine grain size, as observed before. However, in spite of fine grains, the 75% ORp resulted in lower UTS than 50% ORp. From the microstructure of 75% ORp, kissing bond formation was observed that may result in a lower UTS. Along with it some rod shaped secondary particles (as shown in Figure 11c) were also observed that seemed to be accumulated in some particular locations in the nugget zone. The effect of secondary precipitates was also discussed in the previous section. This may have led to coarsening of the particles in that location that made it prone to fail upon tensile loading.
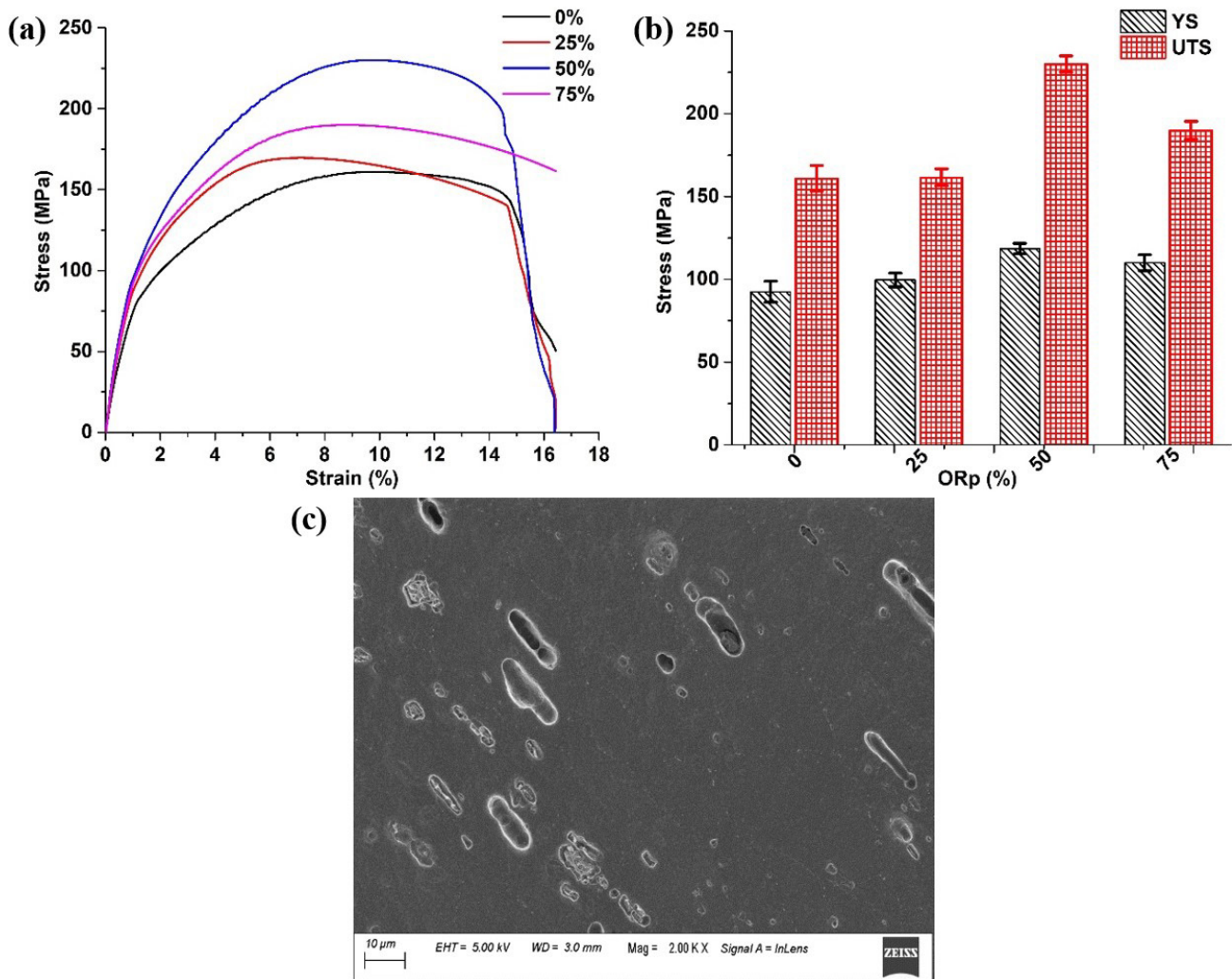

Figure 11. (a) Stress-Strain curve, (b) Average strength at varying ORp and (c) Secondary particles distribution.

For understanding the failure mechanism, the ruptured surfaces of tensile samples were characterized through SEM analysis (Figure 12). It is clear from the figure (both top view and cross-sectional view) that all the samples broke towards the RS. In 0% ORp, the presence of the only flat flakes in fractured surfaces signifies the brittle fracture mode. At the same time, some irregularly shaped dimples with cleavage facets present in the fractured surface of 25% ORp as depicted in the figure, indicates the combined ductile and brittle failure mode. The 50% ORp contains a large population of dimples with different shapes and sizes, as shown. These dimples generally act as voids; their nucleation and growth result in the ductile fracture mode. Mixed-mode failure was observed during 75% ORp, which was denoted by the presence of dimples along with cleavage facets and flat surfaces.

Multi-pass friction stir lap welding of AA 6061-T6: implication of tool pin overlapping on microstructure and mechanical properties of joints

Medhi et al.

ORp **Fracture surface**

Figure 12 Fracture analysis showing various views of fractured samples at varying ORp.

Multi-pass friction stir lap welding of AA 6061-T6: implication of tool pin
overlapping on microstructure and mechanical properties of joints

Medhi et al.

4. Conclusions

The effect of pin overlapping percentage on microstructure and mechanical properties of multi-pass friction stir lap welded AA6061-T6 is reported in the present study. The following points are concluded from the study:

- A simple taper tool without threads was successfully used to fabricate the overlapped joints, and the defects that were earlier present were significantly reduced when the overlapping percentage was increased from 0% to 75%. This suggested that adopting a proper overlapping percentage can help to generate defect-free welds even by using a simple tool geometry;

- Onion rings that were present at low ORp completely disappeared and were replaced by swirl patterns as the ORp increased. This suggested that the overlapping percentage has a distinct effect on the material flow patterns characteristics in the nugget zone;

- Fine equiaxed grains were observed in the nugget zone, the size of which decreases from around 8.5 μm to 3.5 μm with the increase in overlapping percentage, which may be due to experiencing multiple processing of the weld zone. Finer grains were clearly observed in the bottom region as compared to the top region of all the nugget zones created due to multiple passes;

- Random distribution of secondary precipitates in the nugget zone was observed during overlapping from 1st to 5th pass. Particle coarsening due to accumulation was recorded at specific locations at 75% ORp;

- A non-uniform hardness distribution ranging from 43 $HV_{0.1}$ to 49 $HV_{0.1}$ was observed in the combined area of the nugget zone that was significantly lower than that of base metal. A slight increase in hardness values was observed for high overlapping percentage, which may be due to finer grain size achieved. The random distribution of secondary particles due to the stirring led to overall lower and non-uniform hardness distribution in the nugget zone for different ORp;

- The maximum strength of 230 MPa was achieved for 50% overlapping showing the ductile nature of the fracture, and the minimum strength of 160 MPa was achieved for 0% overlapping showing the brittle nature of the fracture. At 75% ORp, though the grains were finer, strength reduced to around 190MPa. This was interpreted due to coarsening of secondary particles in some particular locations in the nugget zone;

- Though 50% ORp showed the highest strength here, a complete parametric study involving varying process parameters along with overlapping conditions is required for more exploration of the area.

References

[1] Sato YS, Kokawa H, Enomoto M, Jogan S. Microstructural evolution of 6063 aluminum during friction-stir welding. Metallurgical and Materials Transactions. A, Physical Metallurgy and Materials Science. 1999;30(9):2429-2437. http://dx.doi.org/10.1007/s11661-999-0251-1.

[2] Feng A, Chen D, Ma Z. Microstructure and low-cycle fatigue of a friction-stir-welded 6061 aluminum alloy. Metallurgical and Materials Transactions. A, Physical Metallurgy and Materials Science. 2010;41(10):2626-2641. http://dx.doi.org/10.1007/s11661-010-0279-2.

[3] Bussu G, Irving P. The role of residual stress and heat affected zone properties on fatigue crack propagation in friction stir welded 2024-T351 aluminium joints. International Journal of Fatigue. 2003;25(1):77-88. http://dx.doi.org/10.1016/S0142-1123(02)00038-5.

[4] Thomas W, Nicholas E. Friction stir welding for the transportation industries. Materials & Design. 1997;18(4-6):269-273. http://dx.doi.org/10.1016/S0261-3069(97)00062-9.

[5] Thomas W. Friction Stir Butt Welding, International Patent Application No. PCT/GB92. GB Patent Application No. 9125978.8. 1991 Dec 6.

[6] Christner B, McCoury J, Higgins S. Development and testing of friction stir welding (FSW) as a joining method for primary aircraft structure. In: 4th International Symposium on Friction Stir Welding; 2003; Park City, Utah, USA. Cambridge: TWI; 2003.

[7] Buffa G, Campanile G, Fratini L, Prisco A. Friction stir welding of lap joints: influence of process parameters on the metallurgical and mechanical properties. Materials Science and Engineering A. 2009;519(1-2):19-26. http://dx.doi.org/10.1016/j.msea.2009.04.046.

[8] Meng X, Cao B, Qiu Y, Chen H, Xie Y, Wan L, et al. Equal-load-bearing joining of alclad AA2024-T4 alloy stringers and skins in aviation via friction stir lap welding. Journal of Manufacturing Processes. 2021;68:1295-1302. http://dx.doi.org/10.1016/j.jmapro.2021.06.043.

[9] Ericsson M, Jin L-Z, Sandström R. Fatigue properties of friction stir overlap welds. International Journal of Fatigue. 2007;29(1):57-68. http://dx.doi.org/10.1016/j.ijfatigue.2006.02.052.

[10] Bisadi H, Tavakoli A, Tour Sangsaraki M, Tour Sangsaraki K. The influences of rotational and welding speeds on microstructures and mechanical properties of friction stir welded Al5083 and commercially pure copper sheets lap joints. Materials & Design. 2013;43:80-88. http://dx.doi.org/10.1016/j.matdes.2012.06.029.

[11] Xu X, Yang X, Zhou G, Tong J. Microstructures and fatigue properties of friction stir lap welds in aluminum alloy AA6061-T6. Materials & Design. 2012;35:175-183. http://dx.doi.org/10.1016/j.matdes.2011.09.064.

Multi-pass friction stir lap welding of AA 6061-T6: implication of tool pin
overlapping on microstructure and mechanical properties of joints

Medhi et al.

[12] Dubourg L, Merati A, Jahazi M. Process optimisation and mechanical properties of friction stir lap welds of 7075-T6 stringers on 2024-T3 skin. Materials & Design. 2010;31(7):3324-3330. http://dx.doi.org/10.1016/j.matdes.2010.02.002.

[13] Astarita A, Tucci F, Silvestri AT, Perrella M, Boccarusso L, Carlone P. Dissimilar friction stir lap welding of aa2198 and aa7075 sheets: forces, microstructure and mechanical properties. International Journal of Advanced Manufacturing Technology. 2021;117(3-4):1045-1059. http://dx.doi.org/10.1007/s00170-021-07816-7.

[14] Zhang Y, Huang Y, Meng X, Li J, Xie Y, Fan Q. Friction stir lap welding of AA2024-T4 with drastically different thickness. International Journal of Advanced Manufacturing Technology. 2020;106(9):3683-3691. http://dx.doi.org/10.1007/s00170-019-04865-x.

[15] Campanella D, Marcon G, Lombardo A, Buffa G, Fratini L. The role of thermal contribution in the design of AA2024 friction stir welded butt and lap joints: mechanical properties and energy demand. Production Engineering. 2022;16(2-3):1-13. http://dx.doi.org/10.1007/s11740-022-01107-0.

[16] Buffa G, Campanile G, Fratini L, Prisco A. Friction stir welding of lap joints: influence of process parameters on the metallurgical and mechanical properties. Materials Science and Engineering A. 2009;519(1-2):19-26. http://dx.doi.org/10.1016/j.msea.2009.04.046.

[17] Kulekci MK, Şik A, Kaluç E. Effects of tool rotation and pin diameter on fatigue properties of friction stir welded lap joints. International Journal of Advanced Manufacturing Technology. 2008;36(9):877-882. http://dx.doi.org/10.1007/s00170-006-0901-z.

[18] Chen Z, Yazdanian S. Friction Stir Lap Welding: material flow, joint structure and strength. Journal of Achievements in Materials and Manufacturing Engineering. 2012;55(2):629-637.

[19] Zhang H, Wang M, Zhang X, Zhu Z, Yu T, Yang G. Effect of welding speed on defect features and mechanical performance of friction stir lap welded 7B04 aluminum alloy. Metals. 2016;6(4):87. http://dx.doi.org/10.3390/met6040087.

[20] Ghosh M, Kumar K, Mishra R. Friction stir lap welded advanced high strength steels: microstructure and mechanical properties. Materials Science and Engineering A. 2011;528(28):8111-8119. http://dx.doi.org/10.1016/j.msea.2011.06.087.

[21] Wang R, Kang H-T, Lei X. Fatigue performance and strength assessment of AA2024 alloy friction stir lap welds. Journal of Materials Engineering and Performance. 2020;29(10):6701-6713. http://dx.doi.org/10.1007/s11665-020-05145-6.

[22] Baratzadeh F, Boldsaikhan E, Nair R, Burford D, Lankarani H. Investigation of mechanical properties of AA6082-T6/AA6063-T6 friction stir lap welds. Journal of Advanced Joining Processes. 2020;1:100011. http://dx.doi.org/10.1016/j.jajp.2020.100011.

[23] Leitao C, Arruti E, Aldanondo E, Rodrigues DM. Aluminium-steel lap joining by multipass friction stir welding. Materials & Design. 2016;106:153-160. http://dx.doi.org/10.1016/j.matdes.2016.05.101.

[24] Osman N, Sajuri Z, Baghdadi AH, Omar MZ. Effect of process parameters on interfacial bonding properties of aluminium-copper clad sheet processed by multi-pass friction stir-welding technique. Metals. 2019;9(11):1159. http://dx.doi.org/10.3390/met9111159.

[25] Leal R, Loureiro A. Effect of overlapping friction stir welding passes in the quality of welds of aluminium alloys. Materials & Design. 2008;29(5):982-991. http://dx.doi.org/10.1016/j.matdes.2007.03.018.

[26] Mishra D, Roy RB, Dutta S, Pal SK, Chakravarty D. A review on sensor based monitoring and control of friction stir welding process and a roadmap to Industry 4.0. Journal of Manufacturing Processes. 2018;36:373-397. http://dx.doi.org/10.1016/j.jmapro.2018.10.016.

[27] Cui G, Ni DR, Ma ZY, Li SX. Effects of friction stir processing parameters and in situ passes on microstructure and tensile properties of Al-Si-Mg casting. Metallurgical and Materials Transactions. A, Physical Metallurgy and Materials Science. 2014;45(12):5318-5331. http://dx.doi.org/10.1007/s11661-014-2494-8.

[28] Muribwathoho O, Msomi V, Mabuwa S, Motshwanedi SS. Impact of multi-pass friction stir processing on microhardness of AA1050/AA6082 dissimilar joints. Materials Today: Proceedings. 2021;46:651-657.

[29] El-Rayes MM, El-Danaf EA. The Influence of multi-pass friction stir processing on the microstructural and mechanical properties of Aluminum Alloy 6082. Journal of Materials Processing Technology. 2012;212(5):1157-1168. http://dx.doi.org/10.1016/j.jmatprotec.2011.12.017.

[30] Zou S, Ma S, Liu C, Chen C, Ma L, Lu J, et al. Multi-track friction stir lap welding of 2024 aluminum alloy: processing, microstructure and mechanical properties. Metals. 2017;7(1):1. http://dx.doi.org/10.3390/met7010001.

[31] Yuqing M, Liming K, Chunping H, Fencheng L, Qiang L. Formation characteristic, microstructure, and mechanical performances of aluminum-based components by friction stir additive manufacturing. International Journal of Advanced Manufacturing Technology. 2016;83(9):1637-1647. http://dx.doi.org/10.1007/s00170-015-7695-9.

[32] Palanivel S, Sidhar H, Mishra R. Friction stir additive manufacturing: route to high structural performance. JOM. 2015;67(3):616-621. http://dx.doi.org/10.1007/s11837-014-1271-x.

[33] Palanivel S, Nelaturu P, Glass B, Mishra RS. Friction stir additive manufacturing for high structural performance through microstructural control in an Mg based WE43 alloy. Materials & Design. 2015;65:934-952. http://dx.doi.org/10.1016/j.matdes.2014.09.082.

[34] Li B, Shen Y, Luo L, Hu W. Effects of processing variables and heat treatments on Al/Ti-6Al-4V interface microstructure of bimetal clad-plate fabricated via a novel route employing friction stir lap welding. Journal of Alloys and Compounds. 2016;658:904-913. http://dx.doi.org/10.1016/j.jallcom.2015.10.288.

Multi-pass friction stir lap welding of AA 6061-T6: implication of tool pin
overlapping on microstructure and mechanical properties of joints

Medhi et al.

[35] Li B, Shen Y, Luo L, Hu W. Fabrication and anti-oxidation properties of Al/Ti-6Al-4V bimetallic clad-sheet by multi-pass friction stir welding. Proceedings of the Institution of Mechanical Engineers. Part B, Journal of Engineering Manufacture. 2015;229(6):1078-1082. http://dx.doi.org/10.1177/0954405414535583.

[36] Mahoney MW, Mishra RS. Friction stir welding and processing. Materials Park: ASM International; 2007.

[37] Fonda R, Bingert J, Colligan K. Texture and grain evolutions in a 2195 friction stire weld. Los Alamos: National Laboratory; 2004.

[38] Buffa G, Hua J, Shivpuri R, Fratini L. Design of the friction stir welding tool using the continuum based FEM model. Materials Science and Engineering A. 2006;419(1-2):381-388. http://dx.doi.org/10.1016/j.msea.2005.09.041.

[39] Nascimento F, Santos T, Vilaça P, Miranda RM, Quintino L. Microstructural modification and ductility enhancement of surfaces modified by FSP in aluminium alloys. Materials Science and Engineering A. 2009;506(1-2):16-22. http://dx.doi.org/10.1016/j.msea.2009.01.008.

[40] Venkateswaran P, Reynolds AP. Factors affecting the properties of Friction Stir Welds between aluminum and magnesium alloys. Materials Science and Engineering A. 2012;545:26-37. http://dx.doi.org/10.1016/j.msea.2012.02.069.

[41] Liu X, Wu C. Material flow in ultrasonic vibration enhanced friction stir welding. Journal of Materials Processing Technology. 2015;225:32-44. http://dx.doi.org/10.1016/j.jmatprotec.2015.05.020.

[42] Mehdi H, Mishra R. Analysis of material flow and heat transfer in reverse dual rotation friction stir welding: a review. International Journal of Steel Structures. 2019;19(2):422-434. http://dx.doi.org/10.1007/s13296-018-0131-x.

[43] Satyanarayana MV, Adepu K, Chauhan K. Effect of overlapping friction stir processing on microstructure, mechanical properties and corrosion behavior of AA6061 alloy. Metals and Materials International. 2020;27(9):1-11.

[44] Krishnan K. On the formation of onion rings in friction stir welds. Materials Science and Engineering A. 2002;327(2):246-251. http://dx.doi.org/10.1016/S0921-5093(01)01474-5.

[45] Oosterkamp A, Oosterkamp LD, Nordeide A. Kissing bond'phenomena in solid-state welds of aluminum alloys. Welding Journal. 2004;83(8):225.

[46] Su J-Q, Nelson TW, Mishra R, Mahoney M. Microstructural investigation of friction stir welded 7050-T651 aluminium. Acta Materialia. 2003;51(3):713-729. http://dx.doi.org/10.1016/S1359-6454(02)00449-4.

[47] Masaki K, Sato YS, Maeda M, Kokawa H. Experimental simulation of recrystallized microstructure in friction stir welded Al alloy using a plane-strain compression test. Scripta Materialia. 2008;58(5):355-360. http://dx.doi.org/10.1016/j.scriptamat.2007.09.056.

[48] Pankaj P, Tiwari A, Biswas P, Gourav Rao A, Pal S. A three-dimensional heat transfer modelling and experimental study on friction stir welding of dissimilar steels. Journal of the Brazilian Society of Mechanical Sciences and Engineering. 2020;42(9):1-27. http://dx.doi.org/10.1007/s40430-020-02556-3.

[49] Chen Y, Ding H, Li J, Cai Z, Zhao J, Yang W. Influence of multi-pass friction stir processing on the microstructure and mechanical properties of Al-5083 alloy. Materials Science and Engineering A. 2016;650:281-289. http://dx.doi.org/10.1016/j.msea.2015.10.057.

[50] Banik A, Saha Roy B, Deb Barma J, Saha SC. An experimental investigation of torque and force generation for varying tool tilt angles and their effects on microstructure and mechanical properties: friction stir welding of AA 6061-T6. Journal of Manufacturing Processes. 2018;31:395-404. http://dx.doi.org/10.1016/j.jmapro.2017.11.030.

[51] Xu W, Liu J, Luan G, Dong C. Microstructure and mechanical properties of friction stir welded joints in 2219-T6 aluminum alloy. Materials & Design. 2009;30(9):3460-3467. http://dx.doi.org/10.1016/j.matdes.2009.03.018.

[52] Dadbakhsh S, Taheri AK, Smith C. Strengthening study on 6082 Al alloy after combination of aging treatment and ECAP process. Materials Science and Engineering A. 2010;527(18-19):4758-4766. http://dx.doi.org/10.1016/j.msea.2010.04.017.